Aqueous tape casting and mechanical properties of $La_2NiO_{4+\delta}$ dense membranes

Xinzhi Chen, Mari-Ann Einarsrud and Tor Grande[1]

Department of Materials Science and Engineering, Norwegian University of Science and Technology, NO-7491 Trondheim, Norway

Abstract

An environmentally friendly aqueous tape casting process for the fabrication of $La_2NiO_{4+\delta}$ membranes was developed using fine powders synthesised by spray pyrolysis. Green tapes with a thickness of 30-300 μm were obtained and dense and homogeneous membranes were prepared by lamination of green tapes followed by sintering in the temperature range 1300-1420 °C. The bi-axial fracture strength of the sintered materials increased from ~ 108 to ~155 MPa decreasing the average grain size of the membranes from about 9.6 to 4.2 μm. The hardness and fracture toughness, measured by the Vickers indentation technique, also decreased with increasing grain size. The mechanical properties of $La_2NiO_{4+\delta}$ ceramics are discussed with focus on micro-cracking/residual stresses due to the strong crystallographic anisotropy of $La_2NiO_{4+\delta}$.

Keywords: $La_2NiO_{4+\delta}$, ceramic membranes, tape casting, mechanical properties

---

[1] Corresponding author: E-mail: grande@ntnu.no

1. Introduction

Gas separation by inorganic membranes is of importance due to their superior mechanical, chemical, and thermal resistance compared with organic membranes [1, 2]. Dense mixed ion and electron conducting (MIEC) membranes can be used to separate oxygen from air with 100 % theoretical selectivity and can also be used as membrane reactors in selective oxidation of light alkanes, such as partial oxidation of methane to syngas [3,4,5] and oxidative dehydrogenation of ethane to ethylene [6]. $La_2NiO_{4+\delta}$ has attracted a significant attention since this material exhibits unique properties, including moderate thermal expansion coefficient, a particularly low chemical expansion and high electrocatalytic activity [7]. $La_2NiO_{4+\delta}$ with the K_2NiF_4-type crystal structure [8] possess a wide range of oxygen hyper-stoichiometry ($0 \leq \delta \leq 0.25$) [9], which is associated with the incorporation of interstitial oxygen ions. The amount of excess oxygen is strongly reduced with increasing temperature and reducing oxygen partial pressure [8]. The low chemical expansion of the material is related to the anisotropic crystallographic expansion of $La_2NiO_{4+\delta}$ which reflects the anisotropy of the crystal structure [7].

The oxygen permeation in $La_2NiO_{4+\delta}$ is not sufficient for membrane reactor design based on thick membranes. To achieve satisfactory oxygen permeation flux it is necessary to decrease the membrane thickness, which gives constraints with respect to the mechanical and chemical stability. Therefore, the fundamental understanding of the mechanical properties of $La_2NiO_{4+\delta}$ is important. To the authors knowledge only Huang et al. have reported the 4-point bending strength of porous $La_2NiO_{4+\delta}$ ceramics [10].

Here, we report on the ceramic processing of dense $La_2NiO_{4+\delta}$ membranes by a combination of aqueous spray pyrolysis and aqueous tape casting. The environmental concerns and health aspects related to the use of organic solvents makes aqueous tape casting attractive. However, the use of water as solvent is more challenging relative to using organic solvents due to problems related to stresses during drying of the tapes [11, 12]. Moreover, we report on the mechanical properties of dense $La_2NiO_{4+\delta}$ membranes. Particular attention is given to the dependence of the grain size since the anisotropic nature of the crystal structure of $La_2NiO_{4+\delta}$ may lead to the development of residual stresses or micro-cracking.

2. Experimental

Membrane preparation

Fine powders of $La_2NiO_{4+\delta}$ (LN) were synthesized by spray pyrolysis of an aqueous precursor solution. Aqueous solutions of the precursors $La(NO_3)_3 \cdot 6H_2O$ (American Elements) and $Ni(NO_3)_2 \cdot 6H_2O$ (Sigma-Aldrich) was prepared, and EDTA (Sigma-Aldrich) was added to the mixture of the two solutions as a complexing agent. The cation content of the two nitrate solutions was determined by a thermogravimetrical analysis and a stoichiometric La:Ni=2:1 ratio were used to in the final precursor solution. The precursor solution was atomized and pyrolysed at 850 °C [13]. The as-synthesized powder was calcined at 800 °C for 8 h in stagnant air followed by ball milling in 100 % ethanol and finally dried and sieved (150 μm) (powder I). Powder I was used for the preparation of the

membranes. A $La_2NiO_{4+\delta}$ powder (powder II) with a larger particle size was processed by an additional calcination of powder I at 1100 °C for 10 h. Powder II was ball-milled and sieved (150 μm) after the second calcination.

Aqueous slips were developed based on the recipe published by Lein et al. [13] and the amount of the different components in the slip recipes are listed in Table 1. Three slips were made with the two different LN powders and two different types of PVA. An overview of the optimized slip preparation process is presented in Fig. 1. The dispersant (Darvan C, R.T. Vanderbilt) was dissolved in distilled water (solution 1) and the LN powder was added to solution 1 and the resulting suspension was dispersion milled (ball mill, ZrO_2 balls) for 6 h forming mixture 1. Solution 2 was prepared by dissolving 15 wt% PVA (PVA-88 (Acros Organics, 88 % hydrolysed, average M.W. 88000) or PVA-115 (VWR, 88 % hydrolysed, average M.W. 115000) in distilled water at 60 °C. Solution 2, the plasticizer polyethylene glycol (PEG) (PEG-10000, Fluka Chemie GmbH), and defoamer polypropylene glycol (PPG) (PPG-2000, Acros organics) were then added to mixture 1, and left for milling for another 12 h with a slow speed forming mixture 2. Additional PPG-2000 was added to mixture 2 and left for further milling for 3 h with a fast speed to remove air bubbles.

Homogeneous slips (no segregation formed after 2 days aging) were cast on a Mylar™ film using a Table Top Tape caster TTC-1200 (Richard E. Mistler, Inc.) with a speed of 10 cm/min and a doctor blade gap of 300 - 750 μm. The tapes were dried on the Mylar film overnight at ambient conditions. To make dense membranes with the required thickness (500 - 800 μm), the green tapes were laminated by pressing a stack of 4 to 6 tapes at 90 –

150 °C for 3 – 5 min at 3 - 4 MPa. Both slip 1 and 2 recipes in Table 1 were used to make the dense membranes. Sheets of approximately 5 × 5 cm^2 were cut from the dried tapes and stacked on top of each other with water sprayed between each tape to aid lamination. The green membranes were heat-treated to remove organic additives for 3 h at 700 °C with a heating rate of 60 K/h up to 200 °C and 30 K/min from 200 to 700 °C, and afterwards sintered in stagnant air at 1300 (LN-1) and 1420 °C (LN-2), respectively. To be able to prepare flat membranes, some of the membranes had to be annealed at 2-300 °C below the sintering temperature between two flat alumina plates after sintering. In addition, pellets (ϕ 20 mm) were also prepared by uniaxial pressing at 25 MPa followed by sintering at 1250, 1300, 1400, 1500 °C for 3 h.

Characterization

The specific surface area of the powders was measured by nitrogen adsorption (Tristar 3000 Micrometrics). The viscosity of the slips after aging was determined using a Haake Mars rheometer (Thermo Scientific). Qualitative X-ray diffraction was carried out with a D8 Focus X-ray diffractometer (Bruker AXS) to confirm the phase purity of the powder and the sintered membranes. The crystallographic density was calculated from the unit cell parameters, determined by Pawley fitting to the data using the orthorhombic space group *Fmmm* [14, 15]. Powder morphology and the microstructure of the membranes and pellets were examined by scanning electron microscopy (SEM) using a Hitachi S-3400 N electron microscope. The cross section of samples were polished to 1 μm and thermally etched at 1150 °C for 30 min. The grain size was measured by the intercept method measuring ~ 100

grains for each sample [16]. The density of the samples was measured by the Archimedes method (ISO 5017) using isopropanol.

The room temperature bi-axial fracture strength of the dense membranes was determined by a ball on ring test [17,18] with a universal mechanical testing machine (Instron 5543). The stress-strain relationship was measured in load control mode until fracture of the specimens, and the stress was calculated using the method described by Chae et al. [17] In total 12 specimens of each membrane type was measured.

Hardness (Hv) and fracture toughness (K_{Ic}) at ambient temperature were measured using Vickers micro-indentation (Leica VMHT MOT) on polished surfaces at a load of 1.96 N. More than 50 indents were measured for each sample. The surface projected diagonal and crack lengths were measured by optical microscopy (a Reickert MeF3 optical microscope with a Sony DXC-930P Colour Video Camera). The fracture toughness was calculated from the average crack length, modulus of elasticity (155 GPa [10]) and measured hardness using the equation described by Malzbender et al. [19].

3. Results

The X-ray diffraction patterns of the as-synthesized powder prepared by spray pyrolysis correspond to the diffraction pattern of $La_2NiO_{4+\delta}$ (Fig. 2), however a small quantity of La_2O_3 was present after calcination at 800 °C. The powder became single phase orthorhombic $La_2NiO_{4+\delta}$ after calcination at 1100 °C or sintering at 1300 °C (Fig. 2).

Powder I calcined at 800 °C had a surface area of 9.4 ± 0.1 m^2/g while calcination at 1100 °C yielded a powder with as surface area of 5.4 ± 0.1 m^2/g. Assuming spherical particles the surface area corresponds to a particle size of 0.09 and 0.16 µm for powder I and II, respectively. Refined lattice parameters for powder I were $a = 5.4614(2)$ Å, $b = 5.4656(5)$ Å and $c = 12.6716(4)$ Å, corresponding to a crystallographic density of 7.03 g/cm^3.

Several slips were prepared from powder I and II according to the procedure outlined in Fig. 1 and all the slips showed pseudoplastic behavior with a viscosity in the range $1800 - 2560$ cP at a shear rate of 50 s^{-1}, which is considered as a similar shear rate as under the doctor blade during casting. [20] Slip 1 (2589 cP at 50 s^{-1}) which contained PVA-88 as the binder showed higher viscosity than slip 2 and slip 3 (2051 cP for slip 2 and 1847 cP for slip 3 at 50 s^{-1}), which were made with PVA-115 as the binder. Successful tape casting was performed only based on recipe 1 and 3. Fully body curl independent on tape thickness was common for the tapes based on recipe 2, indicating that the particle size has a very significant influence on the green tape. The green tapes from slip 1 and 3 had smooth surfaces and a relatively uniform thickness. The thickness of the tapes was in the range $30 - 300$ µm depending on the setting of the doctor blade.

Dense (> 94 %), flat and homogeneous membranes with thickness in the range ($500 - 800$ µm) were obtained after lamination, binder burn-out and sintering. No delimitation of the laminated tapes was observed. Fig. 3 shows the microstructure of the La$_2$NiO$_{4+\delta}$ membranes sintered at 1300 °C (LN-1) and 1420 ºC (LN-2) and the average grain size was 4.2 ± 0.3 µm and 9.6 ± 1.3 µm, respectively. The average grain size and the relative density as a function

of the sintering temperature of the membranes formed by tape casting are compared to the data for the uniaxial pressed pellets in Fig. 4. The relative density of the membranes made by tape casting was lower than that of uniaxial pressed pellets, while the average grain size were slightly larger. Both the relative density and the average grain size increased by increasing the sintering temperature. The materials became dense (> 94 %) at 1300 °C, and the relative density reached a maximum at 1400 °C.

Typical load-displacement curves obtained using the ball on ring test are shown in Fig. 5 and the $La_2NiO_{4+\delta}$ ceramics displayed a close to linear deformation behavior up to fracture. The average calculated fracture strength values were 155 ± 20 MPa and 108 ± 8 MPa for LN-1 and LN-2, respectively showing that the higher sintering temperature resulted in lower fracture strength. Fractography showed a transgranular fracture mode for both membranes (Fig. 4 (a1) and (b1)). The Weibull distribution plots of the mechanical strength data for the membranes are shown in Fig. 6. LN-1 has a Weibull modulus of m = 9 while LN-2 represents a Weibull modulus of m = 17. The higher Weibull modulus for LN-2 suggests that these membranes are more homogeneous even though the strength is lower than for LN-1.

The hardness and the fracture toughness measured by Vickers micro-indentation are plotted as a function of grain size in Fig. 7. The initial increase in the hardness is due to the increasing density. For the dense materials independent on fabrication route, the hardness and estimated fracture toughness decrease with increasing grain size. Optical microscope images of selected indents are shown in Fig. 8. Mainly transgranular cracks are visible from

the corners of the indents independent on grain size in line with the fractography of fracture surfaces. The indentation cracks shown in Fig. 8 are nearly straight for the materials with small grains, while for materials with large grains crack deflection is evident, which is most likely due to the interaction of the cracks with intragranular pores.

4. Discussion

After ball milling and calcination at 800 °C, powder I was not single phase, but with a suitable particle size for excellent tape casting performance, and the final sintered membranes based on powder I was phase pure $La_2NiO_{4+\delta}$ (Fig. 2) according to XRD. Powder II calcined at 1100 °C was phase pure $La_2NiO_{4+\delta}$, but full body curl was common for the green tapes based on this coarser grained powder. Due to the influence of the particle size on tape casting performance it can be concluded that it was not necessary to calcine the as-synthesized powder at 1100 °C to obtain single phase material prior to sintering.

Homogeneous slips could be prepared by careful quality control of the aqueous suspensions. A relatively high viscosity is beneficial to reduce the binder segregations and solid sedimentation [20]. However, the higher the viscosity, the more difficult it is to prepare homogeneous slips. Therefore, a strict quality control was required. Slip 1 and 3 prepared using powder I, but with different types of binder and amount of dispersant, resulted in different slip viscosities. In general, the higher molecular weight of the binder causes higher viscosity. Because the molecular weight of PVA-88 is lower than PVA-115, the mol % of

PVA-88 is higher than for PVA-115 for the same weight %, and the weight % of dispersant in slip 3 was twice the amount in slip 1. This might explain why the viscosity of slip 3 was lower than for slip 1. Green tapes from slip 2 always showed full body curl independent of the thickness (30 – 400 μm) showing that the green tapes are very sensitive to the particle size. One possible explanation of this behaviour is related to the significantly higher observed evaporation rate of the solvent from these tapes. When the surface evaporation rate is faster than the diffusion of solvent in the interior of the green tape, menisci are forced into the green tape creating a capillary pressure. This capillary pressure might cause full body curl of the tape since the top surface of the green tape will experience lateral shrinkage [21]. Tapes from both slip 1 and 3 were used for the fabrication of the dense membranes, yielding dense membranes with similar microstructure and mechanical properties if sintered at the same conditions.

The density and the grain size of the sintered materials were shown to depend on the type of processing technique used. A higher density and a smaller grain size were obtained by uniaxial pressing compared to tape casting. This could be related to two effects: (i) difference in the green density (the relative green density obtained was ~ 32 and ~ 30 % for uniaxial pressed pellets and tape cast membranes, respectively), and (ii) influence of the large aspect ratio of the tape (shrinkage obtained were 36 and 42 % along lateral and vertical direction, respectively). The slight decrease in the density with increasing sintering temperature is due to grain growth accompanied by pore coalescence.

Due to crystallographic anisotropy, the thermal expansion along the c-axis is higher than that along the a-axis for $La_2NiO_{4+\delta}$ [14]. Thus micro-cracking might take place during cooling from the sintering temperature [22]. A number of experimental investigations and theoretical simulations have shown that micro-cracking is significantly related to the grain size for materials with anisotropic crystal structure [23-25]. Since the LN-2 membranes have a larger grain size compared to LN-1 membranes, micro-cracking due to crystallographic anisotropy is more likely to occur in LN-2 samples. However micro-cracking was not evidenced by microscopy of any of the samples (Fig. 3) and the grain size is most likely smaller than the critical grain size for the occurrence of micro-cracking. Residual stresses developed during cooling of the material might however be the reason for the lower hardness, fracture strength and fracture toughness of the LN-2 samples. Huang et al. [10] reported a room temperature flexural strength of ~ 20 MPa for $La_2NiO_{4+\delta}$ samples (52 % porosity). Due to the elimination of residual stress, a 25 % increase of the fracture strength was observed after an annealing process. The importance of small grain size of $La_2NiO_{4+\delta}$ has also been shown to be of importance for enhancing the oxygen flux of membranes [26].

5. Conclusion

A water based tape casting process for fabrication of flat, dense (> 94 %) and homogeneous $La_2NiO_{4+\delta}$ membranes was developed. The type of PVA and the powder particle size had strong influence on the properties of the slips and the quality of the sintered tapes. The biaxial strength was measured to be 155 ± 20 MPa and 108 ± 8 MPa for dense $La_2NiO_{4+\delta}$

membranes with the grain size of 4.2 ± 0.3 μm and 9.6 ± 1.3 μm, respectively. The fracture mode was transgranular in both cases. Vickers micro-indentation revealed a maximum in hardness of ~ 958 MPa before the hardness decreased with the increasing grain size. The estimated fracture toughness, reaching a maximum value of 3.2 ± 0.4 MPa·m$^{0.5}$, was also observed to decrease with increasing grain size. Residual stresses due to crystallographic anisotropy developed in the ceramics during cooling is proposed be the main reason for the observed decrease in hardness, fracture strength and fracture toughness with increasing grain size.

Acknowledgement

References

1. H.P. Hsieh, Inorganic Membranes for Separation and Reaction, Elsevier, Amsterdam, 1996.

2. R. Bredesen, K. Jordal, O. Bolland, High-temperature membranes in power generation with CO_2 capture, Chem. Eng. Process 43 (2004) 1129-1158.

3. J. Sunarso, S. Baumann, J.M. Serra, W.A. Meulenberg, S. Liu, Y.S. Lin, J.C. Diniz da Costa, Mixed ionic-electronic conducting (MIEC) ceramic-based membranes for oxygen separation, J. Membr. Sci. 320 (2008) 13-41.

4. H.J.M. Bouwmeester, Dense ceramic membranes for methane conversion, Catal. Today 82 (2003) 141-150.

5. A. Julbe, D. Farrusseng, C. Guizard, Limitations and potentials of oxygen transport dense and porous ceramic membranes for oxidation reactions, Catal. Today 104 (2005) 102-113.

6. W.S. Yang, H.H. Wang, X.F. Zhu, L.W. Lin, Development and application of oxygen permeable membrane in selective oxidation of light alkanes, Top Catal. 35 (2005) 155-167.

7. V.V. Kharton, A.V. Kovalevsky, M. Avdeev, E.V. Tsipis, M.V. Patrakeev, A.A. Yaremchenko, E.N. Naumovich, J.R. Frade, Chemically induced expansion of $La_2NiO_{4+\delta}$ based materials, Chem. Mater. 19 (2007)2027-2033.

8. L. Minervini, R.W. Grimes, J.A. Kilner, K.E. Sickafus, Oxygen migration in $La_2NiO_{4+\delta}$, J. Mater. Chem. 10 (2000) 2349-2354.

9. V.V. Kharton, A.P. Viskup, E.N. Naumovich, F.M.B. Marques, Oxygen ion transport in La_2NiO_4-based ceramics, J. Mater. Chem. 9 (1999) 2623-2629.

10. B.X. Huang, J. Malzbender, R.W. Steinbrech, Thermo-mechanical properties of $La_2NiO_{4+\delta}$, J. Mater. Sci. 46 (2011) 4937-4941.

11. P. Nahass, W.E. Rhine, R.L. Pober, H.K. Bowen, W.L. Robbins. A comparison of aqueous and non-aqueous slurries for tape casting, Ceram. Trans., vol. 15. Materials and Processes in Microelectronic Systems, Wiley, Westerville, 1990.

12. D. Hotza, P. Greil Review: Aqueous tape casting of ceramic powder, Mat. Sci. Eng. A-Struct. 202 (1995) 206-217.

13. H.L. Lein, T. Tezuka, T. Grande, M.-A.Einarsrud, Asymmetric proton conducting oxide membranes and fuel cells prepared by aqueous tape casting, Solid State Ionics 179 (2008) 1146-1150.

14. S.J. Skinner, Characterisation of $La_2NiO_{4+\delta}$ using in-situ high temperature neutron powder diffraction, Solid State Sci. 5 (2003) 419-426.

15. S.Y. Jeon, M.B. Choi, J.H. Hwang, E.D. Wachsman, S.J. Song, Electrical conductivity and thermoelectric power of $La_2NiO_{4+\delta}$, J. Electrochem. Soc. 158 (2011) B476-B480.

16. N. Das, S. Bandyopadhyay, D. Chattopadhyay, H.S. Maiti, Tape-cast ceramic membranes for microfiltration application, J. Mater. Sci. 31 (1996) 5221-5225.

17. S.-H. Chae, J.-H. Zhao, D.R. Edwards, P.S. Ho, Verification of ball-on-ring test using finite element analysis, 12th IEEE Intersoc. Conf. on Thermal and Thermomech. Phenomena in Electron. Syst. (ITherm) (2010) 1-6.

18. G. de With, H. Wagemans, Ball-on-ring test revised, J. Am. Ceram. Soc. 72 (1989) 1538-1541.

19. J. Malzbender, J.M.J. den Toonder, A.R. Balkenende, G. de With, Measuring mechanical properties of coatings: a methodology applied to nano-particle-filled sol-gel coatings on glass, Mat. Sci. Eng. R 36 (2002) 47-103.

20. R.E. Mistler, E.R. Twiname, Tape casting: Theory and Practice, Wiley, Westerville OH, 2000.

21. T.A. Ring, Fundamentals of ceramic powder processing and synthesis, Academic Press, San Diego 1996.

22. J.A. Kuszyk, R.C. Bradt, Influence of grain size on effects of thermal expansion anisotropy in $MgTi_2O_5$, J. Am. Ceram. Soc. 56 (1973) 420-423.

23. V. Tvergaard, J.W. Hutchinson, Microcracking in ceramics induced by thermal expansion or elastic anisotropy, J. Am. Ceram. Soc. 71 (1988) 157-166.

24. J.J. Cleveland, R.C: Bradt, Grain size/microcracking relations for pseudo-brookite oxides, J. Am. Ceram. Soc. 61 (1978) 478-481.

25. R.W. Rice, R.C. Pohonka, Grain-size dependence of spontaneous cracking in ceramics, J. Am. Ceram. Soc. 62 (1979) 559-563.

26. N. Hildenbrand, P. Nammensma, D.H.A. Blank, H.J.M. Bouwmeester, B.A. Boukamp, Influence of configuration and microstructure on performance of $La_2NiO_{4+\delta}$ intermediate-temperature solid oxide fuel cells cathodes, J. Power Sources 238 (2013) 442-453.

Figure captions:

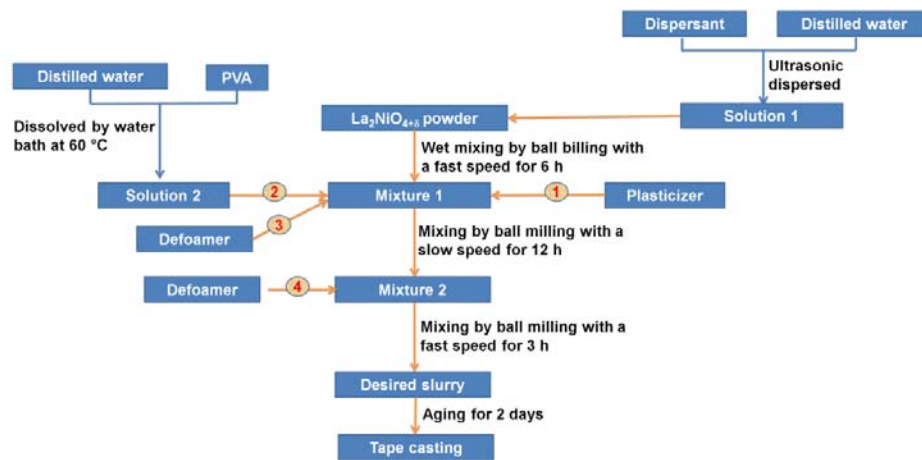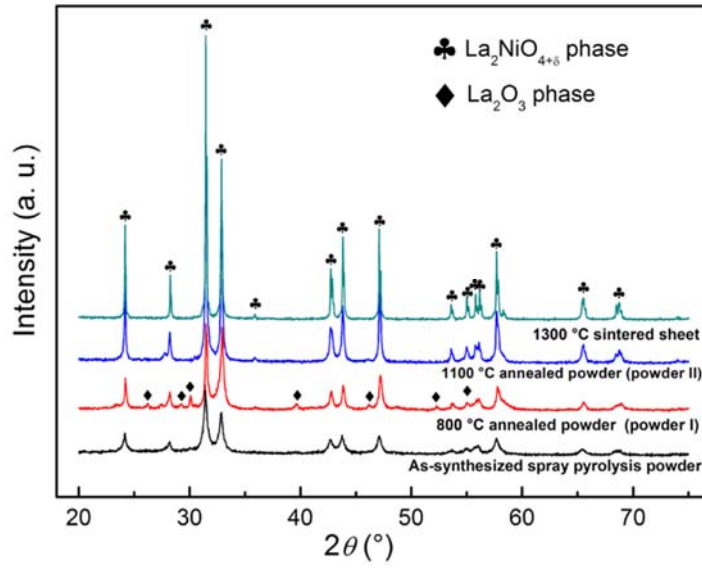**Figure 1.** Process flow for preparation of homogeneous stable $La_2NiO_{4+\delta}$ slips.

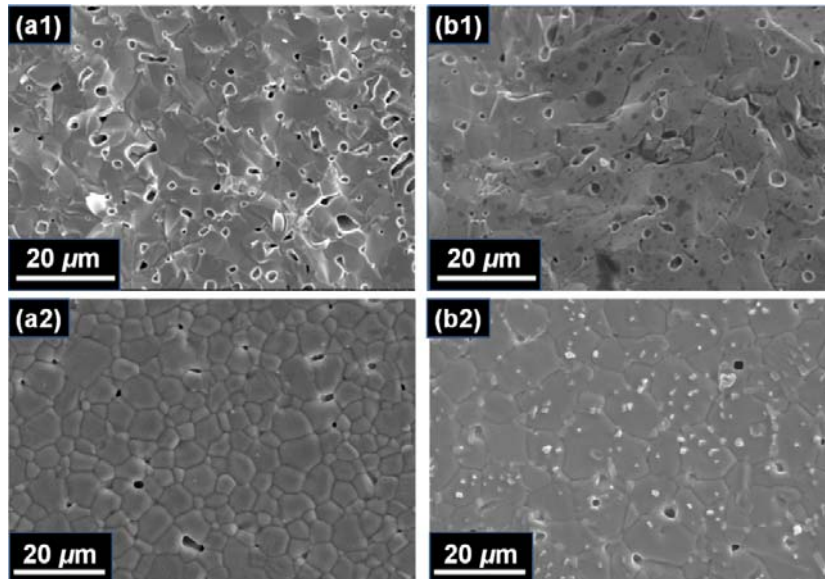**Figure 2.** X-ray diffractograms of $La_2NiO_{4+\delta}$ at the different stages of production.

Figure 3. Representative SEM micrographs of sintered $La_2NiO_{4+\delta}$ membranes (from slip 1 and 3). a) LN-1 sintered at 1300 °C and b) LN-2 sintered at 1420 °C. 1) Fracture surface and 2) polished and thermal etched cross section.

Figure 4. Grain size (a) and relative density (b) of $La_2NiO_{4+\delta}$ pellets and tape cast membranes as a function of sintering temperature.

Figure 5. Typical load-displacement curves of $La_2NiO_{4+\delta}$ membranes tested in ball on ring fracture test. Red dotted line and dark solid lines denote tape cast membranes sintered at 1300 (LN-1) and 1420 °C (LN-2), respectively.

Figure 6. Weibull plots comparing the strength of tape cast $La_2NiO_{4+\delta}$ membranes. LN-1 and LN-2 denote tape cast membrane samples sintered at 1300 and 1420 °C, respectively. *S.T.* and *G.S.* denote sintering temperature and grain size, respectively.

Figure 7. Vickers hardness (a) and fracture toughness (b) of $La_2NiO_{4+\delta}$ pellets and tape cast membranes as a function of grain size.

Figure 8. Optical microscope images of Vickers indents (1.96 N) in $La_2NiO_{4+\delta}$ samples: a) pellet sintered at 1250 °C, b) pellet sintered at 1300 °C, c) pellet sintered at 1400 °C, d) pellet sintered at 1500 °C, e) tape cast membrane sintered at 1300 °C (LN-1), and f) tape cast membrane sintered at 1420 °C (LN-2). Enlargement of selected cracks are placed on the right hand side for the pellet samples and at the bottom for the tape cast membranes.

Table 1. Recipes for the preparation of aqueous $La_2NiO_{4+\delta}$- based slips for tape casting.

Slip No.	1	2	3
LN Powder (wt.%)	28.97 (powder I)	29.12 (powder II)	29.22 (powder I)
Dispersant (wt.%)	0.08	0.13	0.16
Distilled water (wt.%)	62.57	61.81	62.28
Binder (wt.%)	6.33 (PVA-88)	6.83 (PVA-115)	6.36 (PVA-115)
Plasticizer (wt.%)	1.51	1.57	1.48
Defoamer (wt.%)	0.54	0.54	0.50

Figure 1. Process flow for preparation of homogeneous stable La$_2$NiO$_{4+\delta}$ slips.

Figure 2. X-ray diffractograms of La2NiO4+δ at the different stages of production.

Figure 3. Representative SEM micrographs of sintered $La_2NiO_{4+\delta}$ membranes (from slip 1 and 3). a) LN-1 sintered at 1300 °C and b) LN-2 sintered at 1420 °C. 1) fracture surface and 2) polished and thermal etched cross section.
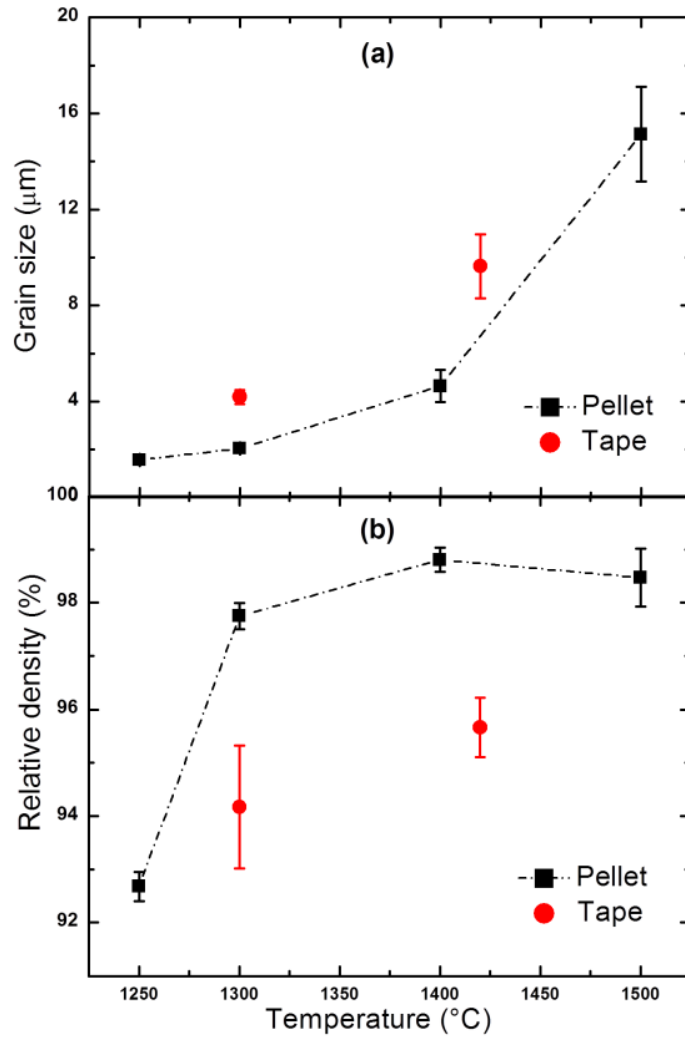
Figure 4. Grain size (a) and relative density (b) of $La_2NiO_{4+\delta}$ pellets and tape cast membranes as a function of sintering temperature.

Figure 5. Typical load-displacement curves of La$_2$NiO$_{4+\delta}$ membranes tested in ball on ring fracture test. Red dotted line and dark solid lines denote tape cast membranes sintered at 1300 (LN-1) and 1420 °C (LN-2), respectively.
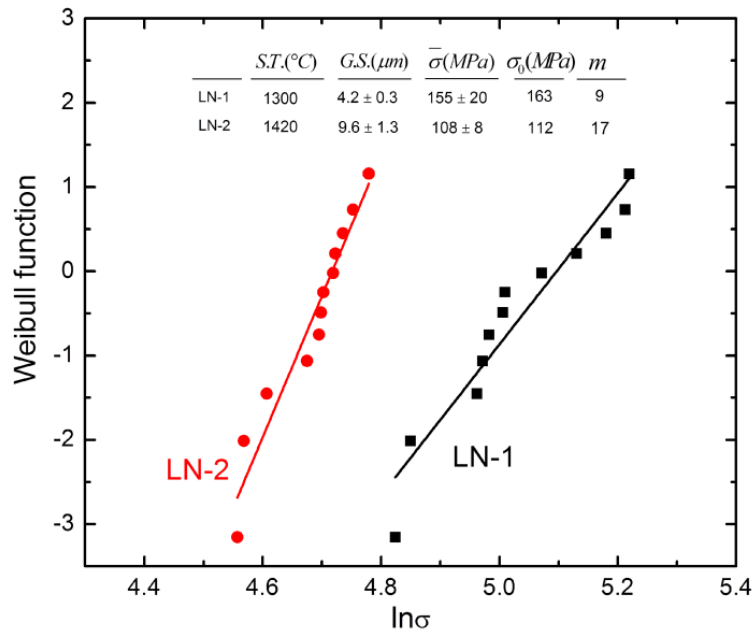
Figure 6. Weibull plots comparing the strength of tape cast $La_2NiO_{4+\delta}$ membranes. LN-1 and LN-2 denote tape cast membrane samples sintered at 1300 and 1420 °C, respectively. *S.T.* and *G.S.* denote sintering temperature and grain size, respectively and $\bar{\sigma}$, σ_0 and m are the average fracture strength, characteristic strength and the Weibull modulus.
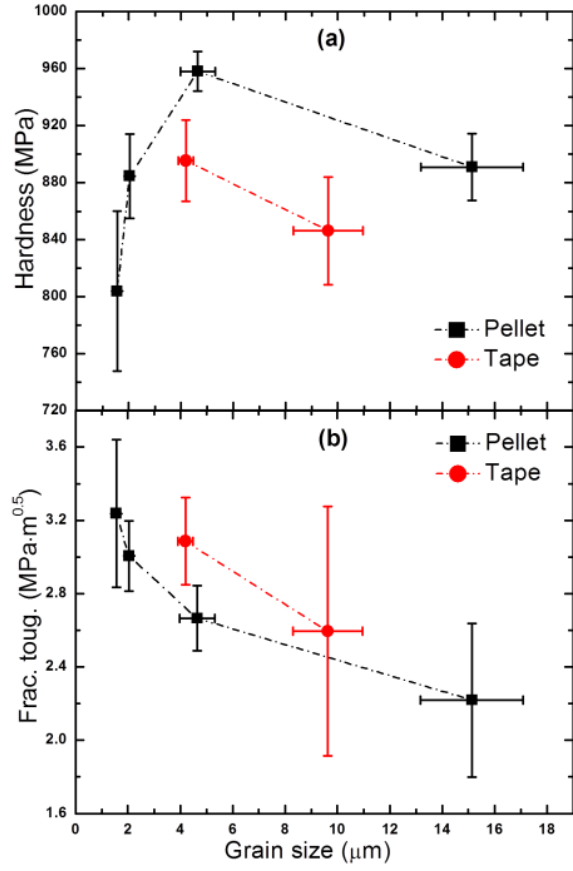
Figure 7. Vickers hardness (a) and fracture toughness (b) of $La_2NiO_{4+\delta}$ pellets and tape cast membranes as a function of grain size.
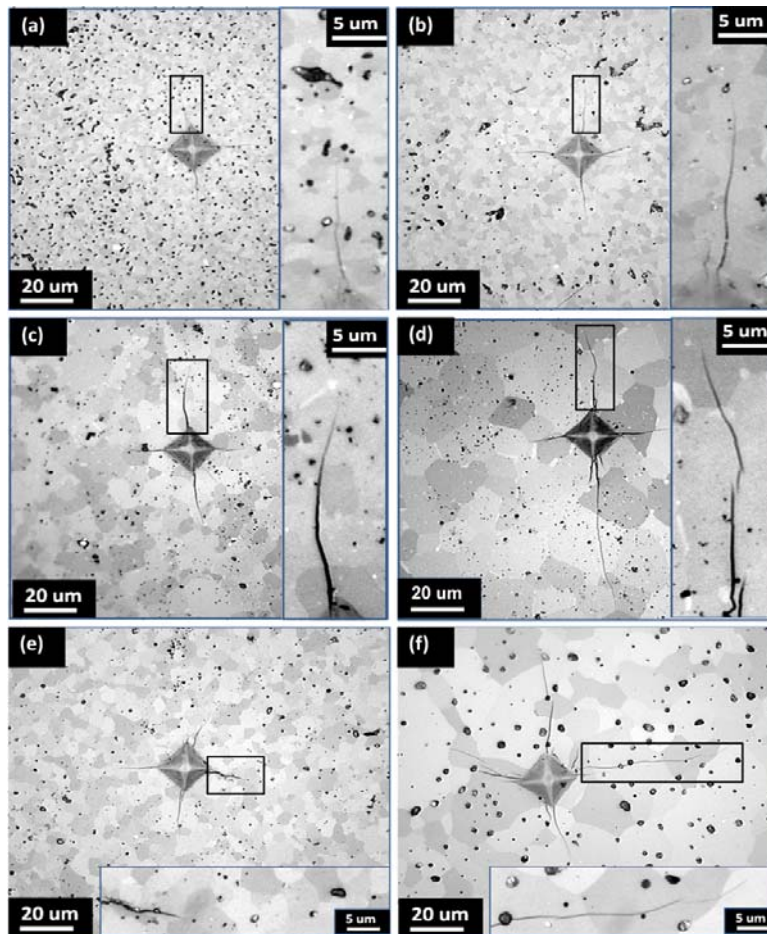
Figure 8. Optical microscope images of Vickers indents (1.96 N) in La$_2$NiO$_{4+\delta}$ samples: a) pellet sintered at 1250 °C, b) pellet sintered at 1300 °C, c) pellet sintered at 1400 °C, d) pellet sintered at 1500 °C, e) tape cast membrane sintered at 1300 °C (LN-1), and f) tape cast membrane sintered at 1420 °C (LN-2). Enlargement of selected cracks are placed on the right hand side for the pellet samples and at the bottom for the tape cast membranes.